Expression of connexin 43 gap junctions and hemichannels following cerebral ischemia in near-term fetal sheep

Carolina Hawranek

Examensarbete januari 2006

Biomedicinsk utbildning
Lunds universitet

Media-Tryck, Kemicentrum, Lund 2006

Master Thesis for MSc in Biomedicine. Lund University, Sweden.
Practical studies completed at the University of Auckland, New Zealand.

Student Research Report. Jan (2006)

Expression of connexin 43 gap junctions and hemichannels following cerebral ischemia in near-term fetal sheep

Carolina Hawranek

Sypervisors: Dr Sherly George, Professor Colin Green and Associate Professor Alistair Jan Gunn.
University of Auckland, New Zealand.
External supervisor: Professor Hakon Leffler, Lund University, Sweden.

Abstract

Connexins are proteins that make up the gap junctions that directly link the intracellular spaces of neighboring cells. Each gap junction is formed by the joining up or docking of two hemichannels in the cell membranes. It has been proposed that the gap junctions themselves or opening of the hemichannels to the extracellular space may allow the spread of cytotoxic signals after injury, leading to progression of cell death. Prolonged, moderate cerebral hypothermia is consistently protective after cerebral ischemia, however, it is unknown whether this therapy affects the expression of gap junctions and their hemichannels. We therefore investigated the time course of expression of connexin 43 gap junctions and hemichannels in white matter after a 30 min episode of cerebral ischemia in term-equivalent fetal sheep. We compared the effect of treatment with brain cooling started 2 h after the ischemic insult and continued until 72 h, which is known to be protective, with cooling delayed until 6 h after ischemia, which has been reported not to reduce white mater injury. Quantification of immunoreactivity was performed with confocal microscopy. The preliminary results indicate that ischemia was associated with a transient increase in both Cx43 and hemichannel expression, maximal at 24 h and resolving by 5 days after ischemia. Intriguingly, hemichannel expression was greater after 5 days in animals that had been cooled from 6h post-insult than those in which cooling was initiated at 2h after the start of ischemia, suggesting that late cooling may not be advantageous, but in fact lead to a delayed induction of connexin expression once the cooling is removed.

1. Background

Severe loss of oxygen and glucose distribution in the brain, termed hypoxia-ischemia, occurs during cardiac arrest, embolic stroke and prenatal asphyxia. This leads to a loss of energy metabolites, subsequent ionic gradient failure and in the most severe cases, cell death.[1,2] Strikingly, however, even after relatively severe insults, there can be a transient recovery of cellular function after return of circulation, although this is followed by progressive expansion of injury into less affected areas of the brain. This delayed failure has been documented in newborn human infants after birth asphyxia, and experimental studies in piglets and fetal sheep have confirmed this evolution, and shown a characteristic 'outward' pattern of spread through different regions.[3-5]

The mechanisms behind this secondary spreading injury are poorly understood but present an opportunity for clinical intervention due to its delayed onset. Since neurons are the first cells to die following ischemia, possibly due to their strictly aerobic metabolism,[6] their abundant synaptic communication has long prompted research to focus on the signaling substances directly causing excitotoxicity.[7] Increasing evidence has suggested that spreading waves of cell depolarization contribute to extending injury, and that these waves may be propagated by direct cell-cell communication via gap junction channels, in the so called "bystander effect". [8,9] More recently, it has been proposed that gap junction hemichannels, or connexons, also play a significant role, by mediating the release of paracrine molecules that propagate cellular death messages,[10] or by opening, thus causing cell swelling (edema).[7]

1.1 Gap junctions: Gap junctions are channels that allow ions and small molecules to pass between adjacent cells. Each is formed from two connexons or hemichannels, which in turn are composed from six proteins called connexins. There are twenty connexin isoforms in the human genome,[11] and they can be recombined to make heteromeric connexons (with more than one connexin isoform per connexon) and heterotypic channels (two different connexons docked together). In the brain the expression of the different connexins varies with region, cell type and developmental stage.[12,13] Connexin 43 is the major connexin expressed by astrocytes and capillary endothelial cells,

Inquiries related to this research project should be adressed to Prof. Colin Green (c.green@auckland.ac.nz) or Assoc. Prof. Alistair Gunn (aj.gunn@auckland.ac.nz).

but also, at lower levels, in microglia.[14,15]

1.2. The gap junction mediated bystander effect: Astrocytes are the most abundant non-neuronal cells in the mammalian brain. Astrocytes regulate the neural environment, maintain potassium, glutamate, pH and extracellular fluid (ECF) volume homeostasis, scavenge free radicals and provide a link between neurons and blood vessels.[16,17] They have long been proposed to supply neurons with substrates for energy production.[27-29] Spatial buffering of factors such as K^+ and glutamate by astrocytes is greatly augmented by coupling through gap junctions,[7,18] thus helping to prevent neurotoxicity. Further, astrocytes closely modulate neurogenesis and synaptic reorganization, which are essential for synaptic recovery after ischaemic injury.[17] Thus, it is perhaps not surprising that changes in astrocytic gap junctions can modulate neuronal survival during and after cerebral ischaemia. Astrocytes are the cell type most highly interconnected by gap junctions and are therefore thought to be an active player in the survival and death of damaged brain tissue. Astrocytes primarily express Cx43, but also Cx30, the second connexin subtype considered unique to astrocytes. In addition Cx26, Cx40 and Cx45 have all been localized on astrocytes although these are also found on other cell types.[12,27] Gap junctions are also found between activated microglia, between many types of neurons, between astrocytes and oligodendrocytes, and possibly between astrocytes and neurons. There is, however, little information on how these gap junctions change after ischaemia, or on how, or whether, they contribute to injury.[7]

Studies supporting a pathogenic role for gap junctions after ischemia report that astrocytes die in clusters following metabolic inhibition[1]. Also, dye transfer studies demonstrate functional coupling of dying and healthy cells.[1] Furthermore, specific knock-down of connexin proteins after local injury significantly reduce damage after ischemia in brain slices[46] and has been shown to accelerate wound repair after skin lesions *in vivo*[47]. The hypothesized spread of cell death by gap junctions has been described in numerous model systems, for reviews see Contreras *et al.*, Krysko *et al.* and Nakase *et al.*[7,10,19]

On the other hand there is also evidence for a protective role of connexins suggesting that connexin expression might mediate both detrimental and advantageous signals depending on the circumstances in the surrounding tissue.[20] A neuroprotective role of connexins is supported by evidence that animals deficient in Cx43 show larger infarct volumes[21,22] and furthermore, increased neuronal death *in vitro* is seen after metabolic inhibition when connexins are blocked pharmacologically.[23]

Although the functional role of connexins remains unclear, several studies have reported changes in connexin expression following ischemia.[24-26] It is established that connexins are essential in several developmental processes[30], but the specific functional roles of the various connexin subtypes are still being evaluated. Mutations in several types have been linked to human disease including the X-linked form of Charcot–Marie–Tooth disease, deafness,[31] and oculodentodigital dysplasia,[32] thus indicating an important role for correct connexin-expression in healthy tissue homeostasis and function.

However, it is important to note that some of the observations ascribed to gap junctions may in fact be mediated by connexin hemichannels.[33] These protein hexamers that form half a channnel in one cell membrane, have been thought to be closed and non-functional until they are docked with an opposing hemichannel thus creating a gap junction. However, emerging evidence suggests that they may be able to open even when unjoined.[34-36] Functional hemichannels *in situ* have been implicated in release of excitotoxic neurotransmitters[36] and hemichannels have been shown to open during metabolic inhibition.[34,35] This could provide a mechanism for paracrine signaling and possibly spreading of cell death.[10]

The majority of studies described above involved *in vitro* models. There are limited data in whole animals, and none on the impact of perinatal ischemic injury on expression of connexin 43 or hemichannels. Thus, in the present preliminary study we examined the time course of expression of connexin 43 and hemichannels in perinatal sheep brains from an *in vivo* global ischemia model. Further, we examined the impact of post-ischemic treatment with hypothermia on expression after 5 days, although we were not able to assess the earlier time course. Further investigation involving larger sample sizes will have to be performed to corroborate and extend the preliminary findings presented in this report.

2. Methods

The present study used tissues from a well described cerebral ischemia model in chronically instrumented fetal sheep at the brain maturational equivalent of term in humans. This paradigm leads to evolving neuronal and white matter damage, in a characteristic watershed pattern.[2,5,37,38] The surgical and experimental procedures were completed previous to the start of the present quantification study.[38]

2.1. Surgical procedures. All procedures were approved by the Animal Ethics Committee of the University of Auckland. In brief, 117-124d of gestation (term= 147days) Romney/Suffolk fetal sheep were anaesthetized with 2% halothane/oxygen, and polyvinyl catheters were placed in both brachial arteries and the amniotic sac. Both carotid arteries were fitted with a double ballooned inflatable occluder cuff, and a 3mm ultrasonic flow probe, just proximal to the cuff. A cooling coil of silicon tubing was wrapped around the head, to the level of the external auditory meatus. To measure fetal temperature a thermistor was placed in the parasagittal dura 20 mm anterior to bregma, and another to measure fetal core body temperature, was placed in

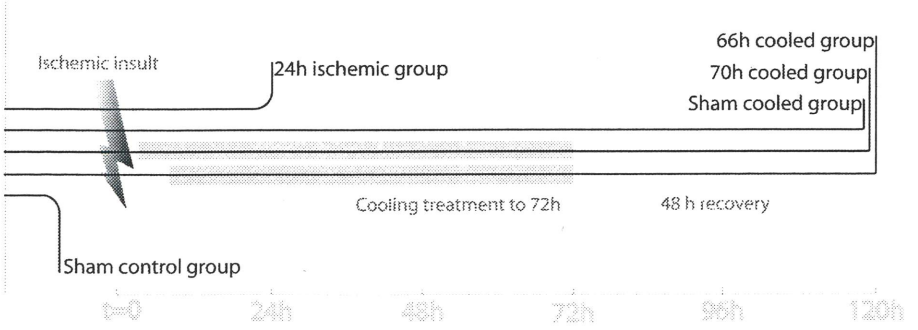

Figure 1: Diagram illustrating treatment groups and sampling times. Each of the five lines represents one treatment group. All brains were fixed and processed in the same way. Sham control group consists of tissue from healthy animals. Damage progression is investigated at 24h (24h ischemic) and at 5 days (sham cooled). All three rightmost groups have undergone the same surgical procedures, but only two groups have been treated with hypothermia starting at 2 or 6 h after the insult.

the esophagus, at the level of the right atrium. Animals were then allowed to recover for several days.

2.2. Experimental procedures: Following 24h of baseline recordings ischemia was induced by inflation of the carotid cuffs around the carotid arteries, thus occluding blood flow in the fetal sheep brain for 30 min. Occlusion was confirmed to be successful by the onset of an isoelectric EEG-signal within 30s of cuff inflation. Fetuses received either no ischemia and no cooling (sham control group), ischemia followed by sham cooling (sham cooled group, and 24h ischemic group), or ischemia followed by cooling initiated 2h or 6h after the start of the ischemic insult and continued until 72 h after ischemia (70h and 66h cooled groups), see Fig. 1 for illustration of treatment groups.

Cooling was executed by connecting the cooling coil to a cold water bath (4 to 10°C) fitted with a circulation pump. The water in the sham cooled group was not circulated, thus the temperature of the cooling coil remained in equilibrium with

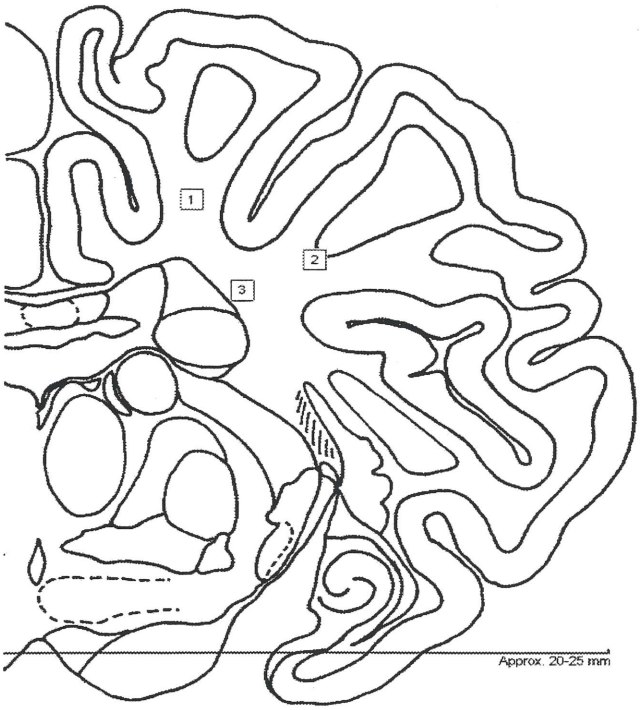

Figure 2: White matter regions sampled in this study. Diagram of a coronal fetal sheep brain section. Area marked "1" is the first parasagittal gyrus, "2" is the second parasagittal gyrus and "3" marks the periventricular white matter.

that of the fetus. Sham cooled ischemia fetuses were put down either 24h or 120 h (5 days) postinsult. All of the fetuses in the two cooling groups were killed after 120 h. All animals were killed by barbiturate overdose. Fetal brains were perfusion-fixed in situ in 10% phosphate-buffered formalin.[2]

2.3. Tissue processing: Experimental brain tissues were paraffin embedded, as follows. Fixed brains were placed in a Tissue Tek VIP 2000 automated processor from Miles Scientific. After dehydration in an increasing strength alcohol series, brains were cleared with chloroform and infiltrated with paraffin wax (Paraplast, tissue embedding medium with a melting point of 56°C, Tyco Healthcare Ltd. UK). Both vacuum and pressure are applied in this process to optimize infiltration of all brain tissue. Following tissue processing, brains were embedded manually on blocks and stored. Coronal sections were obtained by sectioning on a Leica Jung Rm 2035 Microtome. 5µm thick brain slices were sectioned with Extremus low profile disposable mictrotome blades (Proscitech, Australia) and placed on glass microscope slides. Brain sections were finally placed in a heated oven (60-64°C) to help sections adhere to the slides.

2.4. Verification of antibody targets: The synthetic peptide antibody used against Cx43 was obtained from CHEMICON International, Inc. (CA, USA). To investigate the theoretical specificity of the antibody a BLAST search (http://www.ncbi.nlm.nih.gov) was performed with the antigen sequence specified in the Chemicon product sheet (amino acids 252-270 of the mouse Cx43). 100% homology with our target protein in sheep (Ovis aries) was confirmed as well as matches for Cx43 proteins in several other species (hamster, guinea pig, rabbit, mouse). No other matches in sheep were found. The target sequence for the hemichannel antibody was also investigated. A BLAST search confirmed 100% homology with our target sequence in sheep and several other species (human, mouse and hamster). Furthermore, an 80% alignment score (16/20 aa) was found with connexin 44 in sheep, and a 65% alignment score (13/20 aa) was found for Cx26 in sheep.

2.5. Immunohistochemistry: Paraffin embedded brain slices were dewaxed in Xylene, and rehydrated in decreasing strength alcohol series, rinsed in H_2O and washed in PBS. Antigen retrieval was performed by boiling slides in fresh 0.01M citrate buffer, followed by washing in PBS. Slides were then blocked with BBX-solution (0.1M Triton X-100, 0.1M BSA and 200 mM NaCl), for one hour in room temperature. 1:250 primary monoclonal mouse antibody against Cx43 was applied and incubated overnight at 4°C. The following day slides were washed and blocked twice with BBX solution (as above), followed by a three hour incubation with a secondary rabbit anti-mouse fluorescent antibody conjugated with Alexa 488. Finally slides were thoroughly washed in PBS and mounted in CitiFlour antifadant medium (Agar Scientific UK) or Vectashield antifadant medium (Vector Laboratories Inc. Burlinggame, CA, USA). Coronal sections from the same specimens were also stained for Cx43 hemichannels. As for Cx43 labeling, the slides were dewaxed, rehydrated and washed as above. Slides underwent antigen-retrieval by citrate buffer boiling and were then blocked in 2.5% NGS (normal goat serum) for one hour at room temperature. A primary rabbit polyclonal antibody against the first extracellular loop (E1) of mouse Cx43 (kindly provided by Prof. Colin Green) was applied (1:100) and slides were incubated overnight at 4°C. Slides were washed with PBS and a biotinylated (anti-rabbit IgG 1:200) antibody was applied for three hours at room temperature. Slides were again washed in PBS and blocked with BBX-solution for a maximum of 15 min, before a third streptavidin-conjugated Alexa568 antibody (1:200, Molecular Probes, Oregon, USA) was applied and incubated for one hour, in the dark, at room temperature. Finally slides were thoroughly washed in PBS and mounted in Vectashield antifadant medium (Vector Laboratories Inc. Burlinggame, CA, USA).

2.6. Confocal microscopy: Immunoreactivity for connexin 43 and hemichennels was imaged on a Leica SP2 confocal laser scanning microscope. All recordings were obtained blind to treatment. Laser intensity was kept on 25% of maximum (488nm excitation) for Cx43 and 39% of maximum (561nm excitation) for hemichannel detection. Settings were kept consistent during recordings of image series, and any adjustments between batches were carefully recorded. Emission spectrum light was collected in the wavelengths of 500 to 551 nm for Cx43 (Alexa 488) and 570 to 700 nm for hemichannels (Alexa 568). For Cx43 imaging, offset was kept on (-2) for batch 1 and (-3) for batch 2 and gain was kept within a consistent range (750-790) adjusted

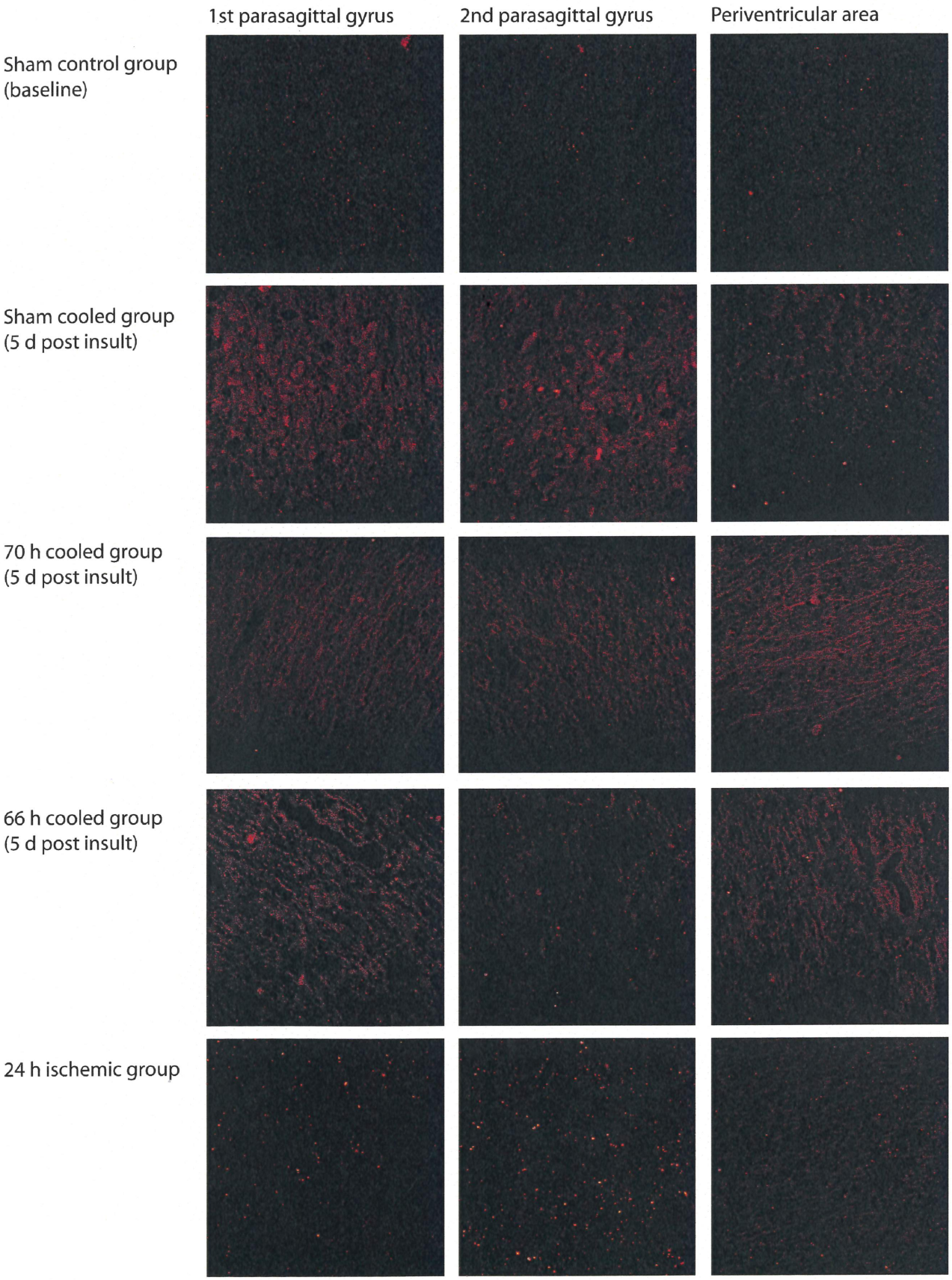

Figure 3: Confocal images of Connexin 43 immunoreactivity (x63) in three areas of the white matter in perinatal sheep brain. Each image is a projection of four focal planes through 3.01μm of brain tissue. Each set of three images (horizontal) is taken from one slide, representative of that treatment group (exceptions for Sham control and 24 post ischemia, were unexplained variations occurred in one case per group). The top set of images shows Cx43 labeling in healthy brain, the bottom set shows Cx43 labeling in ischemic brain 24h after insult. The three middle sets (2-4) show immunolabeling for Cx43 five days after ischemic insult.

only to reduce strong background auto fluorescence in some tissue samples. For hemichannel imaging all series in batch 1 were collected with offset(-3) and gain(430), and batch 2 with offset(-2) and gain(540). Figure 2 shows the areas investigated, which include the white matter in the 1st and 2nd pararasagittal gyrus (PS1, PS2) and the white matter in the periventricular area (PV). Each image series included four focal planes at 63x magnification, through a 3.01µm depth of the brain slice starting about 1µm below the tissue surface. Images were stored in the 1024x1024 pixel format as TIFF-files. All image series for quantification were collected within three days of labeling procedure.

2.7. Image processing; Each series of four focal planes were merged into a Maximum projection using the 3D-projection feature online on the Leica confocal software, or offline on Leica confocal software Simulator SP Version 2.5 (Leica Microsystems Heidelberg GmbH, Germany). Quantification analysis was performed on the projection images.

2.8. Quantification of proteins. The bioimaging software AnalySIS Pro 3.1 (Soft Imaging System GmbH) was utilized to electronically quantify the amount of connexin 43 and hemichannels in the tissue. Again analysis and data collection was performed blind to treatment. The projection of each area was thresholded on a grey-scale image (min:66, max:254 for Cx43 labeling and min:48, max:200 for hemichannel labeling) and detection definition was set to a min of 5 pixels. The total score in each image was recorded.

2.9. Double labeling: To investigate the specific cell populations targeted by our connexin and hemichannel antibodies, a number of double labeling protocols were performed. Brain sections were prepared as detailed for above protocols. Slides to be stained for Cx43 were blocked in BBX and slides to be stained for hemichannels were blocked in 2.5% NGS. Antibodies for Cx43(1:350) and GFAP(1:200), Cx43(1:350) and Tomatolectin(1:50), Hemichannels(1:100) and O4(1:100), Hemichannels(1:100) and NeuN(1:100) were co-incubated overnight at 4°C. Slides were again blocked with appropriate medium before addition of secondary antibodies. The protocols were completed using non cross-reacting fluorescent secondary antibodies (Alexa488), or treated with biotinylated secondary antibodies followed by streptavidin conjugated with Alexa568. Images were collected on a Leica SP2 confocal laser scanning microscope, and the green(488) and red(568) labeling overlayed with the Editing tools online in Leica confocal software (Leica Microsystems Heidelberg GmbH, Germany).

2.10. Data presentation; The data obtained by AnalySIS was sorted into treatment groups and brain regions examined. All data in graphs is presented as mean +/- SEM. Confocal images in this report are presented with enhanced contrast for increased visual clarity.

2.11. Pilot studies; Due to the use of paraffin embedded brain-slices an existing protocol for optimized labeling was not readily available. A comparative trial was performed with connexin-labeling in fresh frozen rat tissue (heart and mouse skin) as positive controls, as these tissues have confirmed high levels of connexin. Further preliminary trials included variations of antibody concentration, antibody type and fluorescent label. The avitin-biotin-amplification proved unnecessary for Cx43 labeling and produced an excessive background staining. A negative control trial excluding the antigen retrieval by citrate boil resulted in virtually total lack of labeling. Further pilot-studies were required to optimize labeling for Cx43 hemichannels. Here, the avidin-biotin amplification proved necessary. All pilot-studies for the final protocols (both Cx-43 and hemichannels) included negative controls treated in parallel omitting the primary antibodies. These slides displayed no punctuate labeling when examined, thus confirming the absence of non-specific label.

3. Results

Fetal sheep (n=20) were subjected to 30 minutes global ischemia and analyzed for parasagittal (PS) and periventricular (PV) connexin and hemichannel expression after 24 hours (n=6) or after five days in a treatment trial (sham, 70 h and 66 h cooled groups). In the treatment trial, sheep underwent head cooling for 70 h (n=4) or 66 h (n=6) following ischemia. As treatment

Sham control group			
Slide #	PS1	PS2	PV
ss1	87	247	16
ss3	44	28	1
ss4	33	3	11
ss5	17	13	15
ss6	1		6
Ave/area	36.4	72.8	9.8
Sham cooled group			
Slide #	PS1	PS2	PV
95/128B		4	4
95/163B			25
95/175C	1		
95/204B	11	6	16
Ave/area	6	5	15
70 h cooled group			
Slide #	PS1	PS2	PV
94/143C			4
95/092A2	37	1	
95/149C	4	8	6
95/176B	4	3	4
Ave/area	15	4	4.67
66 h cooled group			
Slide #	PS1	PS2	PV
96/011C	7	17	
96/018C	22	24	16
96/041C	4		
97/228B	18	9	12
97/246B	2		
Ave/area	10.6	16.6	14
24h isch group			
Slide #	PS1	PS2	PV
03/038C	49	76	39
03/095B	371	338	26
03/100C	53	44	10
03/101B	46	131	15
03/102B	15	49	7
03/103C	15	8	7
Ave/area	91.5	107	17.3

Table 1: Punctate labeling of Cx43 as determined by using AnalySIS. Data was quantified on confocal projections through 3.01µm of brain tissue. Blanks are due to excluded images with compromising artifacts.

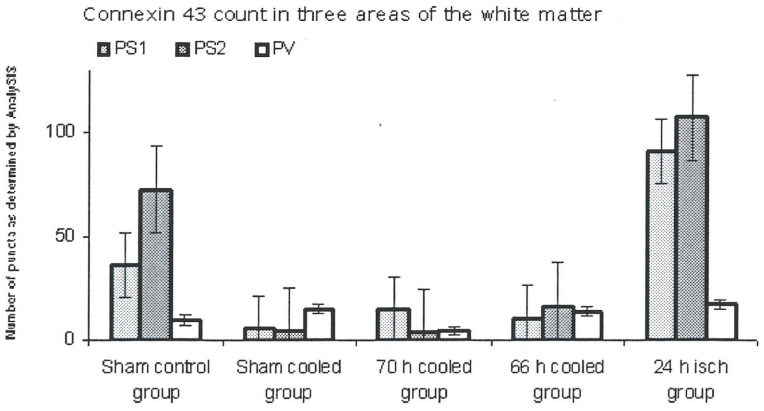

Figure 4: Number of connexin 43 puncta in healthy sheep brain (leftmost group) or in sheep brains following hypoxia-ischemia at 24h (right most group) or five days post insult (three middle groups). Sampling areas include the first and second parasagittal gyrus (PS1 and PS2) and the periventricular white matter (PV). Note that two areas in the control level data and 24h isch level data (PS1 and PS2) are skewed due to the extreme numbers from one slide in each treatment group. Also note the consistently low levels of connexin labeling in the PV area in all treatment groups.

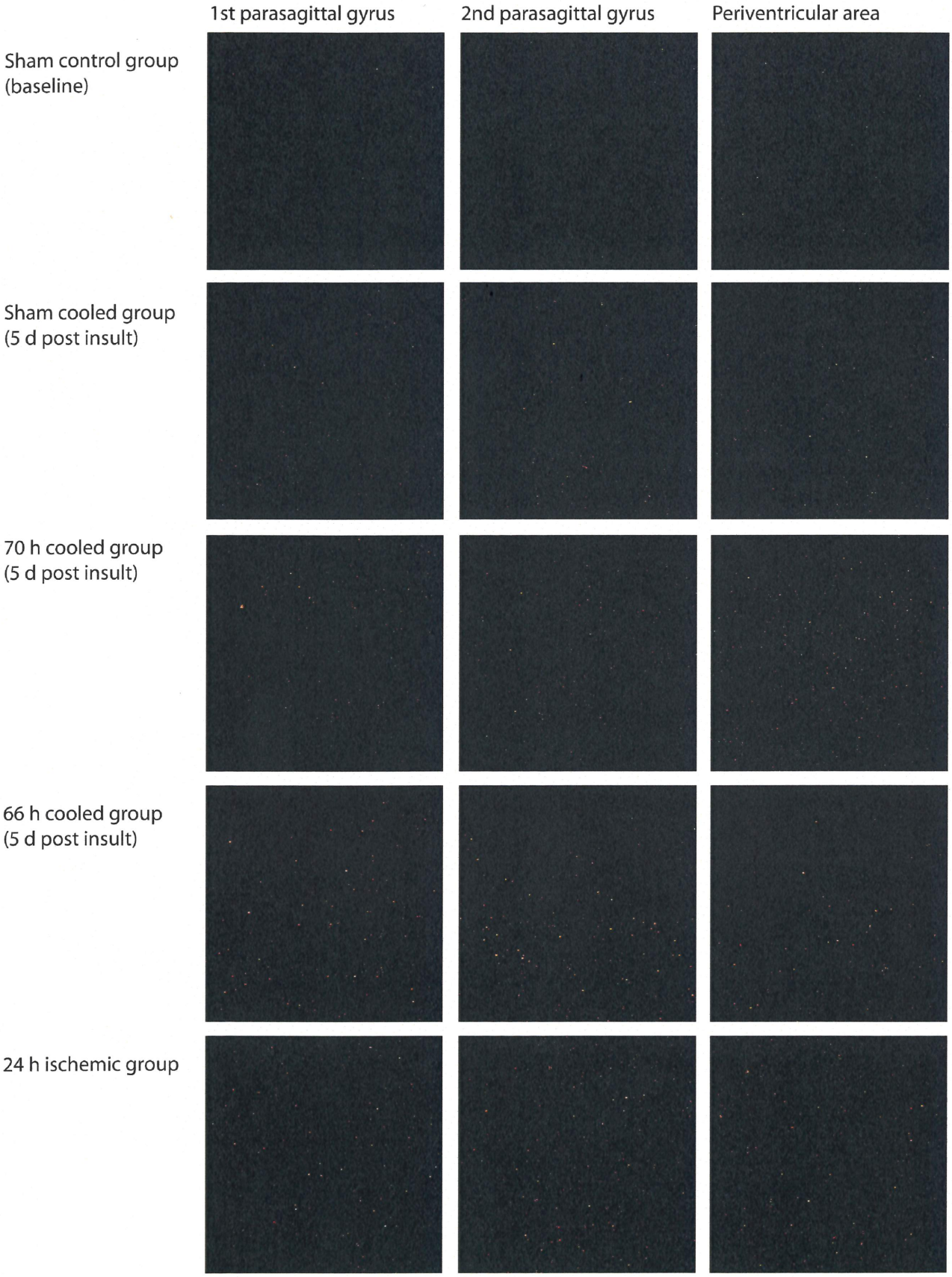

Figure 5: Confocal images of hemichannel immunoreactivity (x63) in three areas of the white matter in perinatal sheep brain. Each image is a projection of four focal planes through 3.01μm of brain tissue. Each set of three images (horizontal) is taken from one slide, representative of that treatment group (exceptions for Sham control group where unexplained variations occurred in one case). The top set of images shows hemichannel labeling in healthy brain, the bottom set shows hemichannel labeling in ischemic brain 24h after insult. The three middle sets (2-4) show immunolabeling for hemichannels five days after ischemic insult.

Sham control group			
Slide #	PS1	PS2	PV
ss1	3	1	5
ss3	165	489	
ss4	0	2	1
ss5	20	30	28
Ave/area	47	130.5	11.3
Sham cooled group			
Slide #	PS1	PS2	PV
95/128B	24	36	15
95/163B	20	25	19
95/175B			
95/204B			
Ave/area	22	30.5	17
70 h cooled group			
Slide #	PS1	PS2	PV
94/143C	40		70
95/092A2	14	6	10
95/149C	17	35	26
95/176B	18	17	62
Ave/area	22.3	19.3	42
66 h cooled group			
Slide #	PS1	PS2	PV
96/011C	62	39	61
96/041C			
97/228B	72	74	35
97/246B	40	52	24
96/092 C	29	27	35
96/023 B	37	80	52
Ave/area	48	54.4	41.4
24h isch group			
Slide #	PS1	PS2	PV
03/038C	56	44	5
03/095B	48	100	60
03/100C	70	99	72
03/101B	142	106	262
03/102B	35	43	71
03/103B	47	68	55
Ave/area	66.33	76.67	87.5

Table 2: Punctate labeling of hemichannels as determined using AnalySIS. Data was quantified on confocal projections through 3.01μm of brain tissue. Blanks are due to excluded images with compromising artifacts.

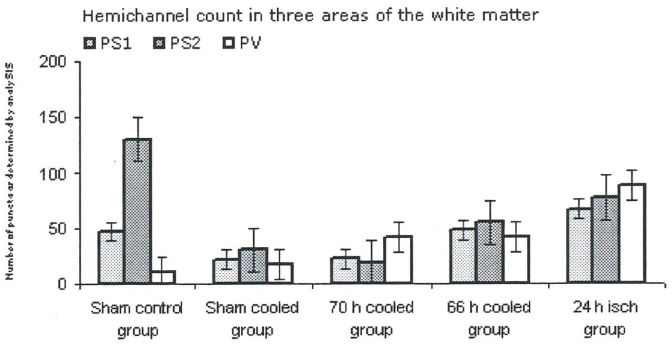

Figure 6: Number of hemichannel puncta in healthy sheep brain (leftmost group) or in sheep brains following ischemia at 24h (right most group) or five days post insult (three middle groups). Sampling areas include the first and second parasagittal gyrus (PS1 and PS2) and the periventricular white matter (PV). Note that part of the control level data (two left most bars) are skewed due to the extreme numbers from one slide. Note also the elevated levels in the "66 h cooled group" as compared to "Sham cooled group" suggesting that cooling initiated too late may delay or even enhance the induction of hemichannel expression after ischemia.

controls, four sheep underwent identical surgical procedures, but recieved no cooling (sham cooled group). As control for baseline expression levels, a fifth treatment group (n=6) with brains from healthy sheep were also analysed (sham control group).

3.1. *Cx43 labeling:* The punctuate labeling for connexin 43 observed by confocal laser scanning microscopy were consistent with earlier descriptions of expression and organization of connexins, as well as size >0.2μm.[39] The panel in Fig. 3 shows examples of images from all treatment groups and areas.

The puncta appeared in a network pattern, suggesting localization of connexin-aggregates to the cell membranes, as is expected for Cx43. Evident artifacts that occurred were air bubbles and disrupted tissue. Compromising factors were clearly distinct from the punctate connexin labeling and affected images were excluded from the quantification analysis.

Fig. 4 and Table 1 summarizes the quantification results of connexin 43 expression. Levels of Cx43 were similar in all treatment groups collected five days after ischemia (sham control, 70h and 66h cooled groups). Connexin-expression was markedly higher at 24h post ischemia, indicating that levels have declined between 24h and 5d after an ischemic insult, as shown. The control group consisting of healthy brains exhibited some unexplained variability in one of the slides, thus skewing the baseline levels.

Due to this variability encountered in baseline data on the parasagittal areas, we cannot with certainty conclude that induction of Cx43 occurred after ischemia, but the preliminary results suggest that baseline levels for this protocol are not substantially different from those five days after the insult. Interestingly, the potential elevation in connexin 43 was limited to the parasagittal white matter while the periventricular white matter displayed a strikingly consistent level of connexin 43 in healthy brain, 24h after ischemia and in all three treatment groups at day five.

Punctate labeling for Cx43 plaques coincided with the pattern of GFAP labeling. Fig. 7 shows a brain section labeled for both Cx43 and GFAP. Double labeling for Cx43 and tomatolectin occurred in separate locations in the white matter (Fig. 8). Lectin labeling was evident in sectioned blood vessels, and did not visibly coincide with punctate labeling for Cx43.

3.2. Hemichannel labeling: Punctate labeling for hemichannels (Fig. 5) was observed to be notably smaller in size, but more wide-spread compared with labeling for Cx43. This was expected since hemichannels may not form plaques as the gap junctional connexin 43 does. As observed in the Cx43 expression data, hemichannel labeling revealed a similar decline in expression levels between 24h and 5d post insult (Fig. 6). Interestingly, however, elevated levels of hemichannels were evident in the "66h cooled group" at day five.

The sham control group includes one slide with markedly elevated data, thus skewing the baseline levels, while all other groups have relatively consistent recordings, as shown in Table 2. Only 7 out of 60 image series in twenty different animals displayed artifacts in the hemichannel protocol. Double labeling for hemichannels and the oligodendrocytic marker (O4) did not display strong enough labeling for conclusive images (data not shown). However, double labeling for the neuronal marker (NeuN) and hemichannels (Fig. 9) showed strong hemichannel stain in the white matter, with significantly less, but detectable labeling in the adjacent cortical regions. The neuronal labeling was clearly limited to cortical areas surrounding the white matter, distinctively labeling neuronal cell bodies and processes.

4. Discussion

The parasagittal white matter areas were chosen to be investigated due to the severe cell loss exhibited in these areas following global ischemia.[2,38] These two areas converge into the periventricular white matter (Fig. 2) which has been observed to exhibit less severe damage.[38] Studies examining progression of cerebral apparent diffusion coefficients after ischemia in the piglet indicate that the secondary wave of energy failure commences in the parasagittal cortex and spreads outward from there in a characteristic pattern.[4] Delayed energy failure have been observed as late as 48h post insult, and in global ischemia in rats, neuronal death has been shown to progress for more than 72 hours after insult[40]. In addition, Gunn et al. have previously shown that it is possible to achieve sustained neuronal and white matter rescue with prolonged head cooling.[2]

In order to compensate for differences in background fluorescence and labeling intensity between animals and between labeling batches several steps were taken. Firstly, to compensate

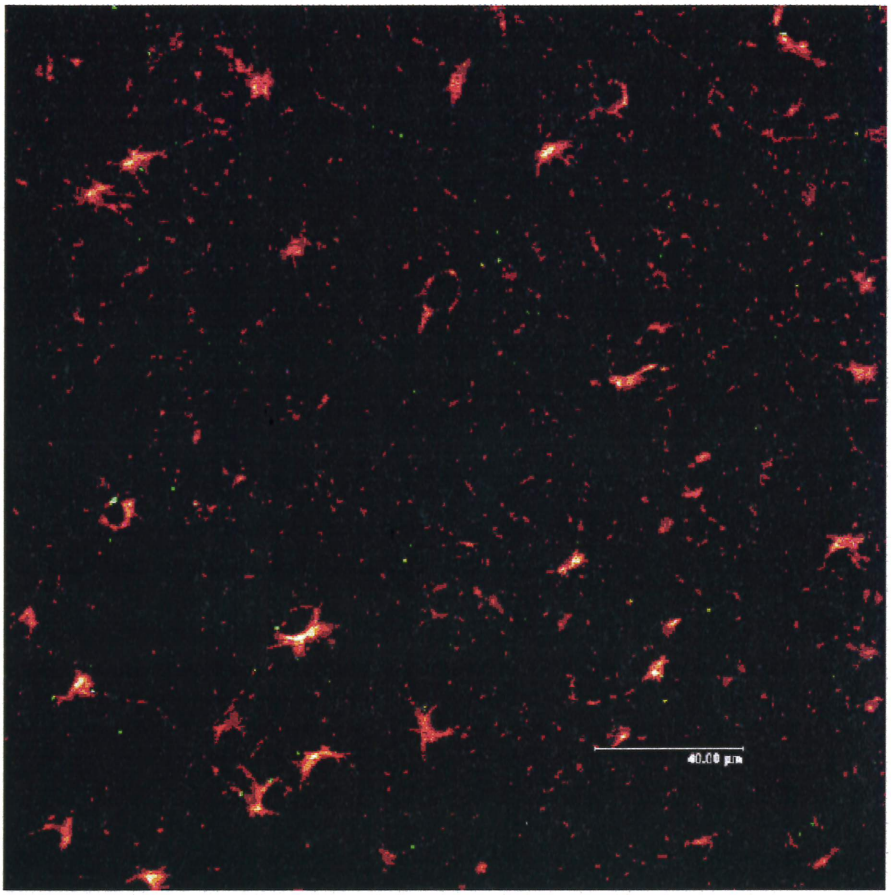

Figure 7: Cx43 staining follows the pattern of astrocytic GFAP. Parasagittal white matter (x63) 24h after hypoxia-ischemia. Red staining shows GFAP and green puncta show Cx43 plaques. Note how the green puncta are located in the cell membranes of near GFAP-stained cells (astrocytes).

for any differences in labeling efficacy between the two batches, duplicate sections were included in both batches, thus allowing us to collect consistent image recordings throughout the analysis. Next, since the quantification was performed by software, the resulting count included all visible light in the images. Therefore, images where artifacts compromised the resulting count were discarded from the quantification data. Finally, and most importantly, the assessment was performed blind to treatment, concurrently with image analysis, enabling an unbiased estimate of connexin levels.

It is important to acknowledge that we found that connexin 43 labeling in paraffin embedded sections was significantly lighter than that of Cx43 in fresh frozen tissues, although paraffinated slides underwent antigen retrieval. The fixation and following tissue processing can significantly alter results of immunostaining studies[12]. Thus it is likely that the punctate labeling recovered by antigen retrieval on the paraffin embedded tissues, is a relative underestimate of connexin 43 in the tissue at the time of fixation. However, with this limitation, the present study enabled us to compare treatment groups

Five days after ischemia, levels of connexin 43 were consistently low in all groups (Fig. 4). This is unlikely to be due to loss of astrocytes, as previous studies using this model have found no change after ischemia, despite severe loss of oligodendroglia.[38] In contrast, after 24h there was a convincingly higher level of labeling overall in this group, as compared with the remaining groups (Table 1 and Fig. 4). As connexin 43 expression is considered abundant in healthy brain, we expected the baseline data from healthy brain to lie between the levels of the 5d post insult groups and the 24h ischemic group. However, the sham controls had greater variability than expected, and therefore the sample sizes are not sufficiently large for us to draw significant conclusions.

Several groups have reported regional discrepancies in labeling of connexins in brain tissue.[12] Immunoreactivity for Cx30 in the white matter regions has been reported to be undetectable in one protocol while other reports have identified Cx30 in astrocytes in the cortical regions[12]. The results were ascribed to the heterogenic expression patterns of connexins in the CNS, and the results we have obtained here might reflect this differential expression. Regional variations in injured brain tissue have also been documented. Severely damaged brain regions do not express much connexins while moderately damaged regions, such as those in ischemic penumbra show highly elevated connexin-levels.[24,25] It is suggested that the type of change and the profile of damage progression is dependent on the severity of the ischemic insult.[40] The rearrangements in connexin expression seem to be an effort by the astroglial syncytium to adapt to changing metabolic demands[25]. Furthermore, detailed characterization of connexin levels in dermal tissue have shown a great plasticity in connexin expression following injury,[14] and human cortical astrocytes exposed to epileptic seizures display increased gap junctional coupling.[41] The variability in connexin data obtained here might therefore be due to regional changes in expression. However, the possibility still exists that the extreme values recorded from single slides might be due to some unintended variation in the labeling protocol, uneven antigen retrieval or an error in the treatment labeling of stored tissues. As we cannot identify the reason for the high numbers in PS1 and PS2 areas (Table 1), further experiments will have to confirm the preliminary findings in these areas.

The periventricular area however, demonstrated remarkably consistent recordings throughout all treatment groups (Fig 4). In fact, previous observations in this sheep model indicate less damage in the periventricular white matter than the strongly affected parasagittal white matter. The unchanged

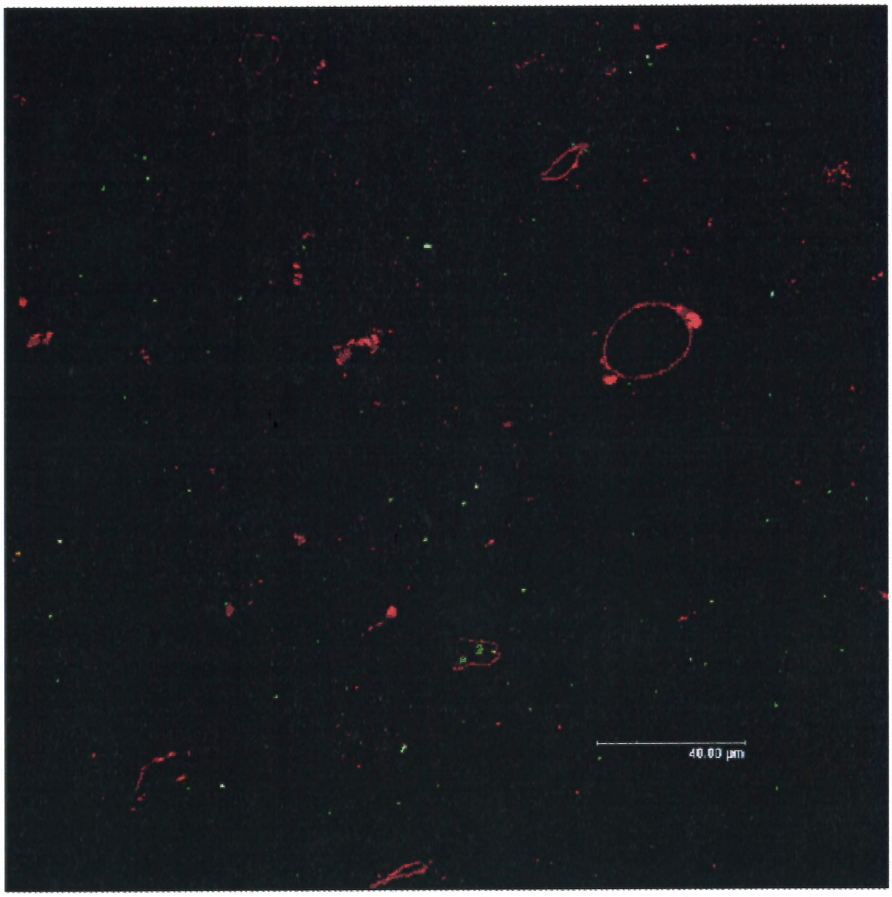

Figure 8: Cx43 staining is located separately from vascular structures and does not appear on activated microglia in this protocol. Parasagittal white matter (x63) 24h after hypoxia-ischemia. Red staining shows immunoreactivity for lectin and green puncta show immunoreactivity for connexin 43 plaques. Note how the green puncta are located separately from the blightly red stained blood vessels.

Cx43 expression in the PV area may be linked to localised differences in cell damage. Furthermore, a few slides displayed what was believed to be vascular labeling, but double label for tomatolectin and Cx43 confirmed that the punctate labeling observed, was different from the labeling of blood vessels, see Figure 8. As tomatolectin also labels activated microglia, and no colocalisation was detected, we conclude that our Cx43 label did not target microglia in this protocol. Double labeling for GFAP and Cx43 was too weak to display clear colocalisation in the overlaid images, but the Cx43 puncta present was observed to occur in the proximity of GFAP-fluorescence (Fig. 7).

The fine punctate labeling of the hemichannels was clearly more abundant in the white matter than in surrounding neuronal regions, but visible in both areas (Fig. 9). The hemichannel antibody used was designed specifically against the first extracellular loop of Cx43, a highly conserved sequence. The E1 and E2 loops include the docking sites required to create a functional gap junction channel, and therefore the antibody is unable to bind to the connexin proteins that have docked to form complete channels. This target sequence is conserved in Cx45 and Cx32, and a BLAST search revealed high alignment scores between our target sequence and Cx 44(80%), as well as Cx 26(65%). The hemichannel labeling is thus not exclusively targeting Cx43 hemichannels, but rather several subtypes of hemichannels as the design intended, likely including Cx43, 45, 32, 44 and 26. This conclusion is supported by the observed fluorescent overlap in sections labeled for neurons and hemichannels (Fig. 9). The colocalised fluorescence for neurons and hemichannels suggests our antibody is targeting hemichannels present on neuronal cell bodies as well as on astrocytes.

The hemichannel labeling in healthy brains contained one slide with very high expression, which remains unexplained, as the three other animals showed consistently low levels of labeling with this protocol (Table 2). As is the case with Cx43 baselines, the hemichannel baseline data will require further studies to validate the normal expression levels in this protocol. However, the remaining groups showed much less variation in hemichannel expression, strongly indicating induction at 24h post insult, which had resolved by 5 days after ischemia (Fig. 6). Interestingly, the expression of hemichannels did not differ between areas as was observed with Cx43. This might be due to the targeting of several hemichannel subspecies, and area specific differences may be masked in this protocol. On the other hand, it is of interest that hemichannel expression in the 66h cooled group was mildly elevated compared with the ischemia alone and 70h cooling groups (Fig. 6). In previous studies even a prolonged phase of cooling, when delayed 6h, did not significant protect the white matter tracts.[38] Thus, speculatively, this may suggest that the cooling treatment initiated 6h after hypoxia-ischemia may have delayed the evolving injury, leading to a corresponding delay in the time course of hemichannel expression after injury.

It has long been questioned why cells would express gap junctions even following injury with such detrimental effects. Indeed, ischemia reduces the coupling of cells effectively after ischemia, but not entirely,[1] which might allow for propagation of cell injury.[42] However, a recent study reports that resistance to injury is conferred by connexin expression unrelated to direct channel function.[30,42] Lin *et al.* demonstrated that the neuroprotective effect of expressing connexin protein was sustained after channel blockage and even when expressing mutant nonfunctional channels. This would explain why many experimental paradigms, including the present *in vivo* study, report increased connexin immunoreactivity in injured brain,[24,25] and yet still be consistent with the observation that the astrocyte

network is partially uncoupled following ischemia.[1,43,44] This dual interpretation of connexin function would also be consistent with the fact that although astrocytes are the most highly coupled cell-type in the brain, they seem more resistant to ischemic injury than neurons.[27] Furthermore, the uncoupling of the astrocyte network following ischemia does not always correlate with losses of connexin abundance. In some studies, the expression levels of Cx43 protein do not change significantly following injury.[26,39] Instead, reports of a reorganization, internalization, and significant remodeling suggest a very dynamic regulation of connexin expression following ischemia.[25,26] It has even been suggested that changes induced by ischemia include novel expression of "stored" connexins.[24] If the neuroprotective effect is not mediated by channel function, the bystander effect observed in dying astrocytes could be an adverse effect of a neuroprotective strategy involving connexin expression. It is conceivable that these neuroprotective levels of connexin protein results in hemichannel expression which might be devastating in the unique circumstances present in the ischemic penumbra. Connexin hemichannels are known to open during metabolic inhibition,[34,35] although they have been shown to have a very low opening probability in healthy cell preparations, this could be altered by ischemic conditions.[45] Only a few open hemichannels can be fatal to the cell.[35] If we consider this possibility in a network of cells expressing Cx43 in abundance, as seems to be the case at 24h after hypoxic-ischemic injury, it is conceivable that hemichannels aggravate the detrimental effects of ischemia in a network already stressed in supporting the metabolic demands of surrounding neurons[27].

5. Conclusions

The preliminary data obtained from our *in vivo* ischemia model are consistent with previous studies showing enhanced connexin-expression in the early period after ischemia.[24,25] The results have shown that a significant decrease in connexin 43 expression occurs between 24h and 5d after ischemic injury and we can speculate that a transient induction of connexin 43 does occur in sheep brain after ischemic injury. Moreover, labeling for Cx43 shows significant differences between closely located brain regions, perhaps reflecting differences in the severity of ischemic damage. In addition we have noted an apparent induction of hemichannel expression in the parasagittal white matter, but more data is required to confirm these findings. Finally, we have recorded differences in hemichannel expression between treatment groups subjected to cooling and the ischemic group, that might indicate that the neuroprotective effect of head cooling is linked to the regulation of hemichannel induction. Further experiments are crucial in order to determine the involvement of connexins and hemichannels in cell death progression.

Acknowledgements

The author would like to thank Alistair Gunn (Dept. of Physiology) for supply of experimental tissues and editorial help, Colin Green (Dept. of Ophtalmology) for continuous practical support and training, Sherly George for assistance in laboratory techniques, Jacqueline Ross, Hilary Holloway and Ratish Kurian (Biomedical Imaging Research Unit) for support on confocal techniques and software, Suzanne Franke (Dept. of Anatomy with Radiology) for advice on antibodies and Lorraine Rolston (Histology laboratory) for tissue preparations. I am also grateful to Michelle Glass (Dept. of Pharmacology) for use of laboratory space and to Hakon Leffler (Department of Molecular Medicine, Lund University) for ecouragement and aid with project registration.

References

1. Cotrina ML, Kang J, Lin JH, Bueno E, Hansen TW, He L, Liu Y, Nedergaard M. Astrocytic gap junctions remain open during ischemic conditions. Journal of Neuroscience 18(7):2520-37, 1998.

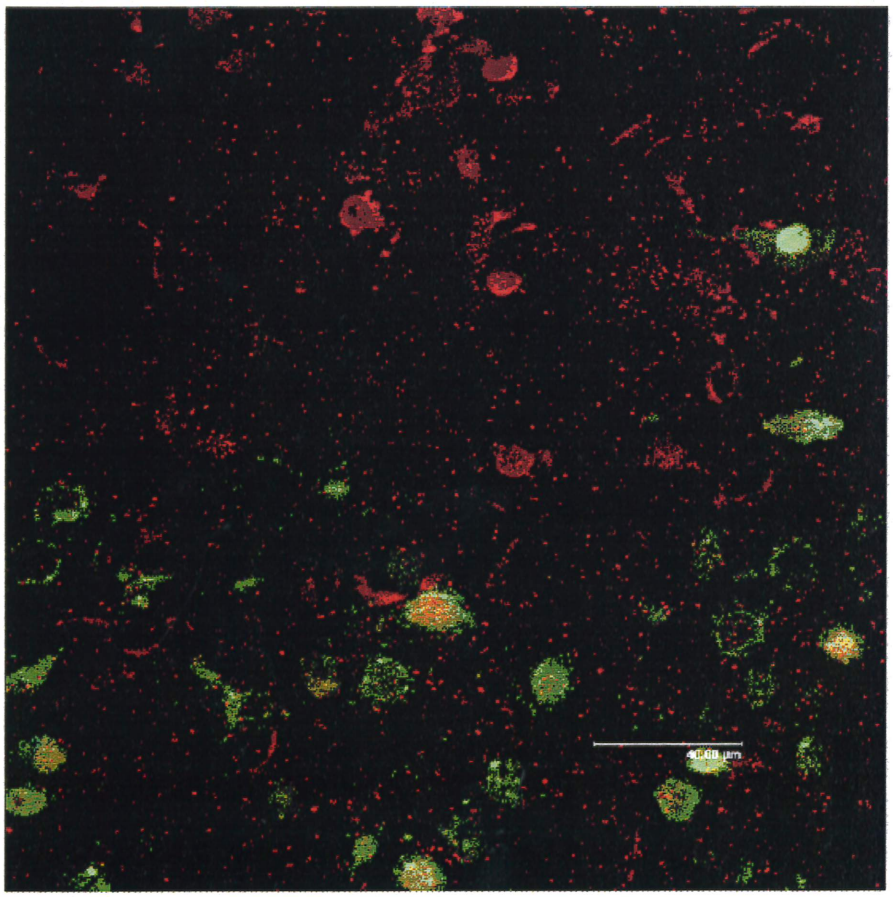

Figure 9: Immunoreactivity for hemichannels and neurons (x63). Image sampled in the border between the parasagittal white matter and adjacent grey matter 24h after ischemia. Red labeling shows hemichannel immunoreactivity and the green label is targeting neurons. Note the yellow overlap on some of the neurons, suggesting that the hemichannel antibody targets hemichannels present on neurons as well as on astrocytes.

2. Gunn AJ, Gunn TR, de Haan HH, Williams CE, Gluckman PD. Dramatic neuronal rescue with prolonged selective head cooling after ischemia in fetal lambs. Journal of Clinical Investigation 99(2):248-56, 1997.
3. Thoresen M, Penrice J, Lorek A, Cady EB, Wylezinska M, Kirkbride V, Cooper CE, Brown GC, Edwards AD, Wyatt JS. Mild hypothermia after severe transient hypoxia-ischemia ameliorates delayed cerebral energy failure in the newborn piglet. Pediatr Res 37(5):667-670, 1995.
4. Thornton JS, Ordidge RJ, Penrice J, Cady EB, Amess PN, Punwani S, Clemence M, Wyatt JS. Temporal and anatomical variations of brain water apparent diffusion coefficient in perinatal cerebral hypoxic-ischemic injury: relationships to cerebral energy metabolism. Magnetic Resonance in Medicine 39(6):920-927, 1998.
5. Williams CE, Gunn A, Gluckman PD. Time course of intracellular edema and epileptiform activity following prenatal cerebral ischemia in sheep. Stroke 22(4):516-21, 1991.
6. Peuchen S, Duchen MR, Clark JB. Energy metabolism of adult astrocytes in vitro. Neuroscience 71(3):855-870, 1996.
7. Contreras JE, Sanchez HA, Veliz LP, Bukauskas FF, Bennett MV, Saez JC. Role of connexin-based gap junction channels and hemichannels in ischemia-induced cell death in nervous tissue. Brain Research - Brain Research Reviews 47(1-3):290-303, 2004.
8. Freeman SM, Abboud CN, Whartenby KA, Packman CH, Koeplin DS, Moolten FL, Abraham GN. The "bystander effect": tumor regression when a fraction of the tumor mass is genetically modified. Cancer Res 53(21):5274-83, 1993.
9. Lin JH, Weigel H, Cotrina ML, Liu S, Bueno E, Hansen AJ, Hansen TW, Goldman S, Nedergaard M. Gap-junction-mediated propagation and amplification of cell injury. Nat Neurosci 1(6):494-500, 1998.
10. Krysko DV, Leybaert L, Vandenabeele P, D'Herde K. Gap junctions and the propagation of cell survival and cell death signals. Apoptosis 10(3): 459-69, 2005.
11. Willecke K, Eiberger J, Degen J, Eckardt D, Romualdi A, Guldenagel M, Deutsch U, Sohl G. Structural and functional diversity of connexin genes in the mouse and human genome. Biol Chem 383(5):725-37, 2002.
12. Nagy JI, Dudek FE, Rash JE. Update on connexins and gap junctions in neurons and glia in the mammalian nervous system. Brain Res Brain Res Rev 47(1-3):191-215, 2004.
13. Sohl G, Odermatt B, Maxeiner S, Degen J, Willecke K. New insights into the expression and function of neural connexins with transgenic mouse mutants. Brain Res Brain Res Rev 47(1-3):245-59, 2004.
14. Coutinho P, Qiu C, Frank S, Tamber K, Becker D. Dynamic changes in connexin expression correlate with key events in the wound healing process. Cell Biol Int 27(7):525-41, 2003.
15. Pepper MS, Montesano R, el Aoumari A, Gros D, Orci L, Meda P. Coupling and connexin 43 expression in microvascular and large vessel endothelial cells. Am J Physiol 262(5 Pt 1):C1246-57, 1992.
16. Lee SH, Kim WT, Cornell-Bell AH, Sontheimer H. Astrocytes exhibit regional specificity in gap-junction coupling. Glia 11(4):315-25, 1994.
17. Chen Y, Swanson RA. Astrocytes and brain injury. J Cereb Blood Flow Metab 23(2):137-49, 2003.
18. Hansson E, Muyderman H, Leonova J, Allansson L, Sinclair J, Blomstrand F, Thorlin T, Nilsson M, Ronnback L. Astroglia and glutamate in physiology and pathology: aspects on glutamate transport, glutamate-induced cell swelling and gap-junction communication. Neurochem Int 37(2-3):317-29, 2000.
19. Nakase T, Naus CC. Gap junctions and neurological disorders of the central nervous system. Biochimica et Biophysica Acta 1662(1-2): 149-58, 2004.
20. Farahani R, Pina-Benabou MH, Kyrozis A, Siddiq A, Barradas PC, Chiu FC, Cavalcante LA, Lai JC, Stanton PK, Rozental R. Alterations in metabolism and gap junction expression may determine the role of astrocytes as "good samaritans" or executioners. GLIA 50(4):351-61, 2005.
21. Nakase T, Fushiki S, Naus CC. Astrocytic gap junctions composed of connexin 43 reduce apoptotic neuronal damage in cerebral ischemia. Stroke 34(8):1987-93, 2003.
22. Ramin Siushansian JFB, David F. Cechetto, Vladimir C. Hachinski, Christian C.G. Naus,. Connexin43 null mutation increases infarct size after stroke. The Journal of Comparative Neurology 440(4):387-394, 2001.
23. Blanc EM, Bruce-Keller AJ, Mattson MP. Astrocytic Gap Junctional Communication Decreases Neuronal Vulnerability to Oxidative Stress-Induced Disruption of Ca2+ Homeostasis and Cell Death. Journal of Neurochemistry 70(3):958-970, 1998.
24. Hossain MZ, Peeling J, Sutherland GR, Hertzberg EL, Nagy JI. Ischemia-induced cellular redistribution of the astrocytic gap junctional protein connexin43 in rat brain. Brain Res. 652(2):311-22, 1994.
25. Li WE, Ochalski PA, Hertzberg EL, Nagy JI. Immunorecognition, ultrastructure and phosphorylation status of astrocytic gap junctions and connexin43 in rat brain after cerebral focal ischaemia. Eur J Neurosci. 10(7):2444-63, 1998.
26. Martinez AD, Saez JC. Regulation of astrocyte gap junctions by hypoxia-reoxygenation. Brain Research Reviews 32(1):250-258, 2000.
27. Kirchhoff F, Dringen R, Giaume C. Pathways of neuron-astrocyte interactions and their possible role in neuroprotection. European Archives of Psychiatry & Clinical Neuroscience 251(4):159-69, 2001.
28. Tsacopoulos M. Metabolic signaling between neurons and glial cells: a short review. Journal of Physiology-Paris 96(3-4):283-288, 2002.
29. Tsacopoulos M, Magistretti P. Metabolic coupling between glia and neurons. J. Neurosci. 16(3):877-885, 1996.
30. Lin JH, Yang J, Liu S, Takano T, Wang X, Gao Q, Willecke K, Nedergaard M. Connexin mediates gap junction-independent resistance to cellular injury. Journal of Neuroscience 23(2):430-41, 2003.
31. Simon AM, Goodenough DA. Diverse functions of vertebrate gap junctions. Trends in Cell Biology 8(12):477-483, 1998.
32. Vasconcellos JP, Melo MB, Schimiti RB, Bressanim NC, Costa FF, Costa VP. A novel mutation in the GJA1 gene in a family with oculodentodigital dysplasia. Arch Ophthalmol. 123(10):1422-6, 2005.
33. Saez JC, Contreras JE, Bukauskas FF, Retamal MA, Bennett MV. Gap junction hemichannels in astrocytes of the CNS. Acta Physiol Scand. 179(1):9-22, 2003.
34. Contreras JE, Sanchez HA, Eugenin EA, Speidel D, Theis M, Willecke K, Bukauskas FF, Bennett MV, Saez JC. Metabolic inhibition induces opening of unapposed connexin 43 gap junction hemichannels and reduces gap junctional communication in cortical astrocytes in culture. Proceedings of the National Academy of Sciences of the United States of America 99(1):495-500, 2002.
35. John SA, Kondo R, Wang S-Y, Goldhaber JI, Weiss JN. Connexin-43 Hemichannels Opened by Metabolic Inhibition. J. Biol. Chem. 274(1): 236-240, 1999.
36. Ye Z-C, Wyeth MS, Baltan-Tekkok S, Ransom BR. Functional Hemichannels in Astrocytes: A Novel Mechanism of Glutamate Release. J. Neurosci. 23(9):3588-3596, 2003.
37. Gunn AJ, Williams CE, Mallard EC, Tan WK, Gluckman PD. Flunarizine, a calcium channel antagonist, is partially prophylactically neuroprotective in hypoxic-ischemic encephalopathy in the fetal sheep. Pediatric Research 35(6):657-63, 1994.
38. Roelfsema V, Bennet L, George S, Wu D, Guan J, Veerman M, Gunn AJ. The window of opportunity for cerebral hypothermia and white matter injury after cerebral ischemia in near-term fetal sheep. J Cereb Blood Flow Metab 24(8):877-886, 2004.
39. Oguro K, Jover T, Tanaka H, Lin Y, Kojima T, Oguro N, Grooms SY, Bennett MV, Zukin RS. Global ischemia-induced increases in the gap junctional proteins connexin 32 (Cx32) and Cx36 in hippocampus and enhanced vulnerability of Cx32 knock-out mice. Journal of Neuroscience 21(19):7534-42, 2001.
40. Colbourne F, Li H, Buchan AM, Clemens JA. Continuing Postischemic Neuronal Death in CA1 : Influence of Ischemia Duration and Cytoprotective Doses of NBQX and SNX-111 in Rats • Editorial Comment: Influence of Ischemia Duration and Cytoprotective Doses of NBQX and SNX-111 in Rats. Stroke 30(3):662-668, 1999.
41. Lee SH, Magge S, Spencer DD, Sontheimer H, Cornell-Bell AH. Human epileptic astrocytes exhibit increased gap junction coupling. Glia. 15(2):195-202, 1995.
42. Lin JH, Weigel H, Cotrina ML, Liu S, Bueno E, Hansen AJ, Hansen TW, Goldman S, Nedergaard M. Gap-junction-mediated propagation and amplification of cell injury.[see comment][erratum appears in Nat Neurosci 1998 Dec;1(8):743]. Nature Neuroscience 1(6):494-500, 1998.
43. Daniel Hinkerohe DS, Aiden Haghikia, Katharina Heupel, Claus G. Haase, Rolf Dermietzel, Pedro M. Faustmann,. Effects of cytokines on microglial phenotypes and astroglial coupling in an inflammatory coculture model. Glia 52(2):85-97, 2005.
44. Faustmann PM, Haase CG, Romberg S, Hinkerohe D, Szlachta D, Smikalla D, Krause D, Dermietzel R. Microglia activation influences dye coupling and Cx43 expression of the astrocytic network. GLIA 42(2):101-8, 2003.
45. Contreras JE, Saez JC, Bukauskas FF, Bennett MV. Gating and regulation of connexin 43 (Cx43) hemichannels. Proceedings of the National Academy of Sciences of the United States of America 100(20):11388-93, 2003.
46. Frantseva MV, Kokarovtseva L, Perez Velazquez JL. Ischemia-induced brain damage depends on specific gap-junctional coupling[erratum appears in J Cereb Blood Flow Metab. 2003 Feb;23(2):261.]. Journal of Cerebral Blood Flow & Metabolism. 2002;22:453-462.
47. Qiu C, Coutinho P, Frank S, Franke S, Law LY, Martin P, Green CR, Becker DL. Targeting connexin43 expression accelerates the rate of wound repair. Current Biology. 2003;13:1697-1703.